ENGINEERING TRANSACTIONS • *Engng. Trans.* • **50**, 4, 305–322, 2002
Polish Academy of Sciences • Institute of Fundamental Technological Research
10.24423/engtrans.534.2002

THEORETICAL AND EXPERIMENTAL INVESTIGATIONS OF BRAKING ENERGY RECOVERY IN AUTOMOBILES AND HEAVY MACHINERY

J. OCIOSZYŃSKI

Warsaw University of Technology,
Faculty of Automobiles and Heavy Machinery Engineering
84 Narbutta Str.
02-524 Warsaw

The paper deals with theoretical computations and experiments concerning the possibility of energy recuperation in certain phases of automobile and heavy machinery driving cycles as well as in working cycles of heavy machinery working mechanisms.

1. Introduction

It follows from the literature analysis [1, 2, 3] that the energy saving (recovering) is most frequently related to automobiles with electric drive systems or to automobiles with hybrid electromechanical drive systems. In these vehicles the energy is saved by the electric systems, where the kinetic energy of braking is transformed into electric energy. The saved electric energy (electric drive motor works as a generator) is stored in electrochemical batteries to insignificantly extend the vehicle range, or it supplies the resistance units and in this way is used as an additional source of heat.

The presented possibilities to recover or accumulate the braking energy of hybrid or electrically driven vehicles put forward the idea to use this energy in classically driven heavy machinery. The kinetic energy of braking, transformed by a direct-current generator into electric energy, can also supply storage batteries or resistors in classically driven vehicles and heavy machinery. Furthermore, in heavy machinery the potential braking energy, produced during lowering the loaded sheave blocks (i.e. cranes), may be recovered and transformed into electric energy and used to supply the electrochemical batteries or loading resistors [4].

The research on vehicle and machinery braking energy recovery or recovery of the potential energy of the load and work equipment is usually carried out at model stands. The tests made on real objects are time-consuming and expensive procedures and do not provide for generalisation of the results. The model tests, on the contrary, enable to carry out a wide range of experiments, and thanks to the presumed mechanical and electrical scale factors, cover the whole range of produced automotive vehicles and heavy machinery.

In the case of automobiles, the test stand (with low voltage) presented in Fig. 1 was used. The mathematical model was created to test simulation systems on the basis of the belonging to the test stand equipment electric machines characteristics [5] (Fig. 1), with a special attention paid to the control system and self-excited direct-current machine with serial excitation system working as a current generator. The mathematical model was used for numerical simulation of an automotive vehicle electrodynamic braking with energy recuperation. The recovered energy was supplied to the load resistors and electrochemical battery.

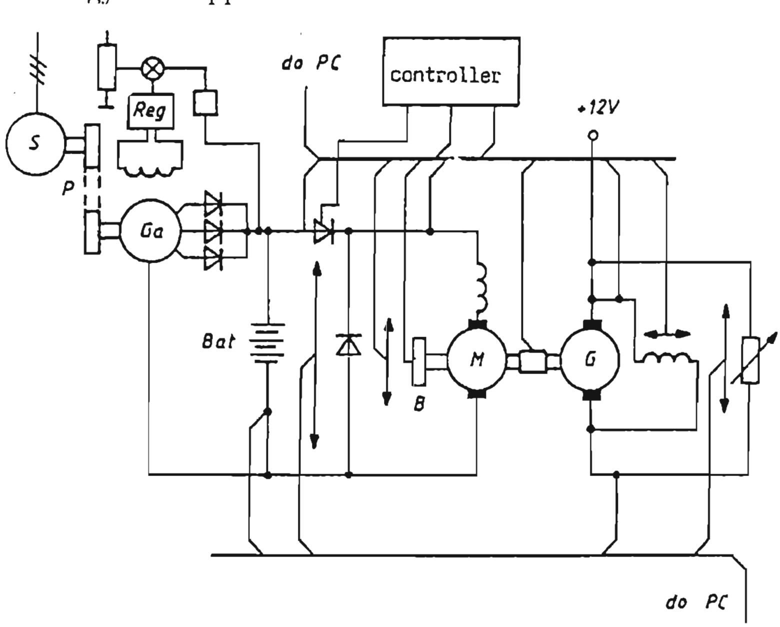

FIG. 1. Schematic diagram of the model stand (low voltage) S – 4 kW electric machine, $\omega = 153.8\ s^{-1}$, $U = 380/220$ V, P – double belt transmission of 2.8 ratio, G_a – alternator with power of 1.5 kW, $U = 36$ V, $\omega = 439.6\ s^{-1}$, Bat – electrochemical battery unit $U = 36$ V, M – series direct-current machine with power of 1.6 kW, $U = 36$ V, $\omega = 293\ s^{-1}$, B – rotating mass simulating vehicle mass (mass = 96 kg, radius = 205 mm), G – direct-current generator (shunt or separately excited) with loading regulation elements, Reg – controlled feeder of alternator induction circuit.

Verification of the simulations was carried out on the model stand with resistors and electrochemical batteries supplied by the recovered energy. Real experiment series on automotive vehicles braking energy were carried out using the model stand (medium voltage) shown in Fig. 2 [6]. Energetic properties of the stand correspond to a certain overload of mechanical into electrical energy transducer (direct-current generator). For this reason, the results of experiments relate to the wide scope of values of mechanical and electrical units. The control and measuring system are provided for experiment automation according to the presumed parameters. The block scheme of the stand [7] for the tests and measurements of energy to be recovered during braking phases of the working mechanisms and drive cycles of heavy machinery is presented in Fig. 3. The experiments were carried out for a self-propelled crane.

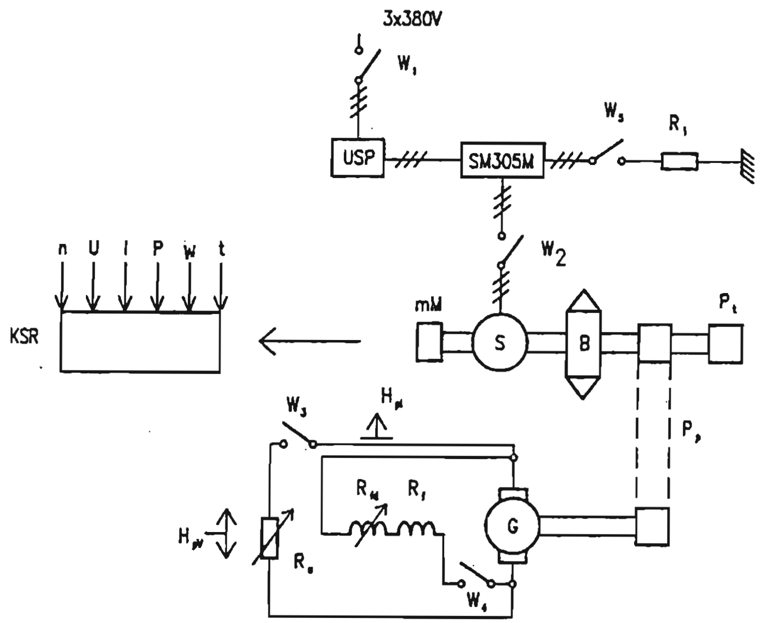

FIG. 2. Schematic diagram with direct-current generator (medium voltage) USP – control and measuring system, SM305M – controller, R_1 – additional load resistor (brake), S – alternative current machine, B – inertia mass, mM – torque meter, P_t – tachometer generator, P_p – belt transmission, G – direct-current generator, R_f – generator excitation coil, R_{fd} – excitation circuit additional resistor, R_o – generator load resistance, H_{pi}, H_{pu} – current and voltage halothrone transducer, $w_1 \div w_5$ – switches, KSR – computer register system, n – rotational speed, U – generator terminals voltage, I – generator load current, P – generator load power, W – energy transmitted to load resistor, t – experiment time.

The gross energy produced at a single braking phase depends on automotive vehicle or machinery mass and the initial braking speed (drive cycle), or it depends on the mass of loaded sheave block and weight lowering time (working mechanisms duty cycle). However, the net energy amount (the energy to be used) is much less than the gross amount, as the mechanical to the electrical energy transformation assumes small values. This was confirmed by energy tests per-

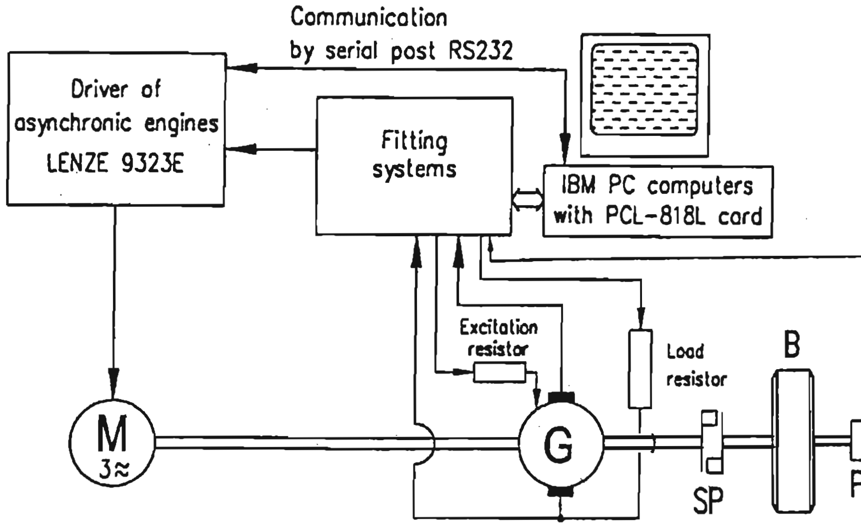

FIG. 3. Block diagram of the test stand M – alternative current machine, G – direct-current generator, SP – clutch, B – inertia mass, PT – tachometer generator.

formed on model test stands. Since recent years, only the recovered energy has been considered in the power balance of vehicle and heavy machinery with classical drive systems. The additional energy became indispensable to fulfil severe criteria, such as:

- energy savings during the whole period of vehicle or heavy machinery exploitation,
- decrease of emission of solid and gas exhausts pollution substances.

In particular, when an intensive protective activity of environment is observed, the second criterion occurred to be the most vital and inspired numerous practical ideas. Automotive vehicles and heavy machinery with Diesel engines are the source of harmful solid substances (soot). The soot itself is not harmful, but benzopyrene is adsorbed on it (3,4-benzopyrene is a carcinogenic exhaust component, very dangerous to the humans). On the engine outlet systems, solid particles filters are installed to lower the soot emission to the atmosphere. The recovered energy will be utilised for filters regeneration – to burn out the soot deposits.

The recuperated energy transformed into electrical energy supplies the load resistors of the generator, which produce a large amount of heat. The energy supplied to the filter increases the soot temperature up to its spontaneous ignition temperature (about 900 K). For this purpose, the generator load heating resistors capable of radiating the heat energy of 3 – 5 MJ are utilised.

2. Simulation tests of vehicle braking energy and model stand validation

Using components and units of the model stand (Fig. 1) on the basis of the determined machine characteristic properties and the stand control system, the mathematical model for simulation tests of vehicle braking energy (energy recuperation) was formulated. It may be stated on the basis of the detailed analysis of the scheme given in Fig. 1 that direct-current self-excited series machine is supplied by electrochemical battery where a T – type impulse converter is used.

The corresponding scheme of this part of the model stand is presented in Fig. 4. The electrical circuit method with the second Kirchhoff law was applied, in accordance with [8], for the analysis of the electric machine dynamic states.

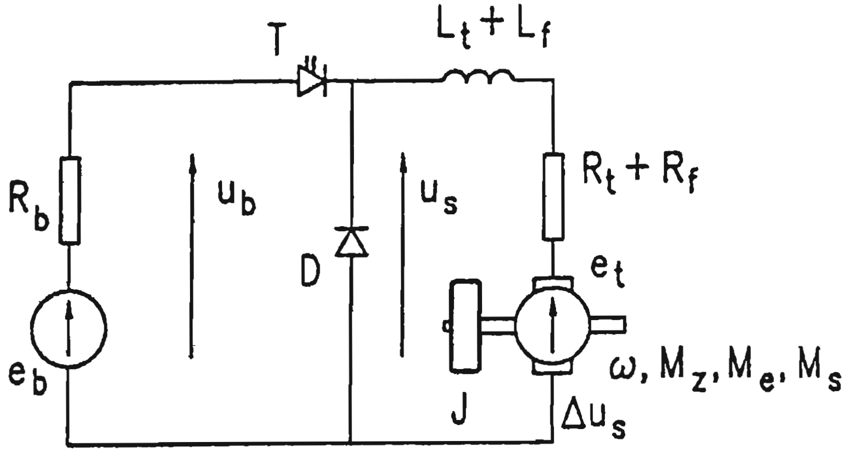

FIG. 4. Schematic diagram of self-excited series direct-current machine in experimental stand configuration for start-up phase e_t – actual value of machine armature electromotive force, $R_t + R_f$ – resistance of armature and excitation coil, $L_t + L_f$ – inductance of armature and excitation coil, T – impulse converter, D – rectifying diode, R_b – battery internal resistance, e_b – actual value of battery electromotive force, u_b – actual value of battery voltage, ω – armature angular speed, M_z, M_e, M_s – momenta: external, electromagnetic, system losses, J – inertia momentum, u_s – actual voltage on machine termianals, Δu_s – brush voltage drop.

In this case, the model of series electrical machine dynamics is described in the literature by equations of voltages and torques with consideration of additional elements shown in the scheme (Fig. 4). It should be considered in electrical machine systems supplied by electrochemical batteries, that the battery voltage decreases during the load increase. The voltage drop generated at the brushes is also considered. The self-excited series direct-current electrical machines work at high electromagnetic parameters what causes saturation of the magnetic current. For this reason, the conjugate magnetic flux formulation is used in voltage equation instead of the constant inductance approach. In accordance with the above mentioned assumptions, the equations may be written as follows:

$$
\begin{aligned}
& e_t - \left(N_t \frac{\partial \phi_t}{\partial i_t} + N_f \frac{\partial \phi_f}{\partial i_t} \right) \frac{di_t}{dt} - (R_t + R_f) i_t - \Delta u_S(i_t) - \Delta u_T(i_t) = u_b, \\
& e_t = c\, \phi\,(i_t)\, \omega\,(t), \\
& u_b = e_b(i_t,\, t) \;-\; R_b i_b, \qquad\qquad (2.1)\\
& J\, \frac{d\omega}{dt} = M_e - M_S - M_Z, \\
& M_e = \; c\, \phi\,(i_t)\, i_t\,,
\end{aligned}
$$

where i_t – armature current, i_b – battery current, t – time, Δu_T – voltage drop at the conductive converter, N_t, N_f – coil number of armature and excitation windings.

The T converter (Fig. 4) enables impulse regulation of mean voltage at the drive motor terminals. The output voltage of the converter depends on pulse – width modulation (PWM) factor α:

$$\alpha = \frac{t_1}{T_1} \qquad (2.2)$$

where: t_1 – converter conduction time, T_1 – pulse repetition period.

The current i_b is governed by the following equation if the converter system stabilises the current i_t at a certain level:

$$i_b = \alpha\, i_t \qquad (2.3)$$

in which α changes within the interval $\alpha_{\min}$ to 1.

The electric machine work process modelling demands two sets of equations depending on the converter switching state. These states are defined by the step function:

$$f_p\,(i_t) = 1 \quad \text{for} \quad i_t \leq\, i_A - 0,5\, \Delta i_t\,, \qquad (2.4)$$

$$f_p\,(i_t) = 0 \quad \text{for} \quad i_t \geq\, i_A + 0,5\, \Delta i_t\,, \qquad (2.5)$$

where: Δi_t – assumed amplitudes of armature current, i_A – input value of armature current.

For the converter switching at state ($f_p = 1$), the equations of the electric machine are as follows:

$$\frac{di_t}{dt} = \frac{1}{N_t \frac{\partial \phi_t}{\partial i_t} + N_f \frac{\partial \phi_f}{\partial i_t}} \left[c\phi(i_t)\omega - \right.$$

(2.6)
$$\left. (R_t + R_f) i_t - \Delta u_T - \Delta u_S - e_b + R_b i_b \right],$$

$$\frac{d\omega}{dt} = \frac{1}{J}\left[c\phi(i_t) i_t - M_S - M_Z\right].$$

For the converter switching-off state ($f_p = 0$), the equations may be given in the form:

(2.7)
$$\frac{di_t}{dt} = \frac{1}{N_t \frac{\partial \phi_t}{\partial i_t} + N_f \frac{\partial \phi_f}{\partial i_t}} \left[c\phi(i_t)\omega - (R_t + R_f) i_t - \Delta u_D\right],$$
$$\frac{d\omega}{dt} = \frac{1}{J}\left[c\phi(i_t) i_t - M_S - M_Z\right],$$

where Δu_D– voltage drop at diode D.

Schematic diagram of the direct-current self-excited series machine installed at the test stand for braking phase differs from the scheme presented in Fig. 4 by the following features:

there is a rectifying diode installed to pass the current to braking energy receivers, instead of the T converter,

a thyristoric converter is used instead of the diode D for machine shortage and current passage in armature coil – this is an activation phase of generator operation of the machine.

The set of equations describing generator operation of the machine for $f_p = 1$ is as follows:

(2.8)
$$\frac{di_t}{dt} = \frac{1}{N_t \frac{\partial \phi_t}{\partial i_t} + N_f \frac{\partial \phi_f}{\partial i_t}} \left[c\phi(i_t)\omega - (R_t + R_f) i_t - \Delta_{U_S} - \Delta u_D\right],$$

$$\frac{d\omega}{dt} = \frac{1}{J}\left[c\phi(i_t) i_t - M_S - M_Z\right].$$

For the converter switch-off state with $f_p = 0$, the equations are as follows:

$$\frac{di_t}{dt} = \frac{1}{N_t \frac{\partial \phi_t}{\partial i_t} + N_f \frac{\partial \phi_f}{\partial i_t}} \left[c\phi(i_t)\omega - \right.$$

(2.9)
$$\left. (R_t + R_f) i_t - 2\Delta_{U_D} - \Delta_{U_S} - e_b - R_b i_b \right],$$

$$\frac{d\omega}{dt} = \frac{1}{J}\left[c\phi(i_t) i_t - M_S - M_Z\right].$$

For the braking phase when the energy is passed to resistor $e_b = 0, R_b = R$.

The simulation tests of energy recuperation deal with energy storage in electrochemical 34 Ah battery and passing it to resistors for different angular speeds of series direct-current generator starting at 293 s^{-1}. The tests were made for batteries with discharge factor equal to 0.1, 0.2, 0.3, 0.4, 0.5 and load resistance limited by 0.1 – 0.4 Ω.

Table 1 shows the test results for energy storage in battery, while Table 2 contains the tests results for energy passage to the resistors. Figure 5 shows the graph of energy recuperation efficiency versus the battery discharge factor.

Table 1. Results of simulation studies of braking energy transmitted to electrochemical battery versus generator angular speed and 34 Ah battery discharge factor.

Change of angular speed s^{-1}	Time of tests s	Change of energy value kJ	Energy recuperation value kJ	Energy recuperation efficiency	Accumulator discharge ratio
293 40.6	68	86.0 1.65	48.5	0.564	0.1
293 40.5	68	86.0 1.63	48.5	0.576	0.2
293 40.2	68	86.0 1.62	48.6	0.577	0.3
293 40.4	68	86.0 1.63	48.7	0.577	0.4
293 40	68	86.0 1.61	48.7	0.577	0.5

Table 2. Results of simulation studies of braking energy transmitted to resistors versus generator angular speed and load resistance.

Change of angular speed s^{-1}	Time of tests s	Change of energy value kJ	Recuperated energy kJ	Energy recuperation efficiency	Load resistance [Ω]
293 57.5	0 48	86.0 3.6	24.3	0.319	0.40
293 56.5	0 49	86.0 3.1	34.5	0.450	0.35
293 51.1	0 56	86.0 2.9	43.2	0.560	0.30
293 41.3	0 62	86.0 2.9	48.2	0.620	0.25
293 35.7	0 37	86.0 2.2	49.3	0.630	0.23
293 34.5	0 32	86.0 1.6	38.8	0.490	0.20
293 27.5	0 18	86.0 0.5	17.5	0.220	0.10

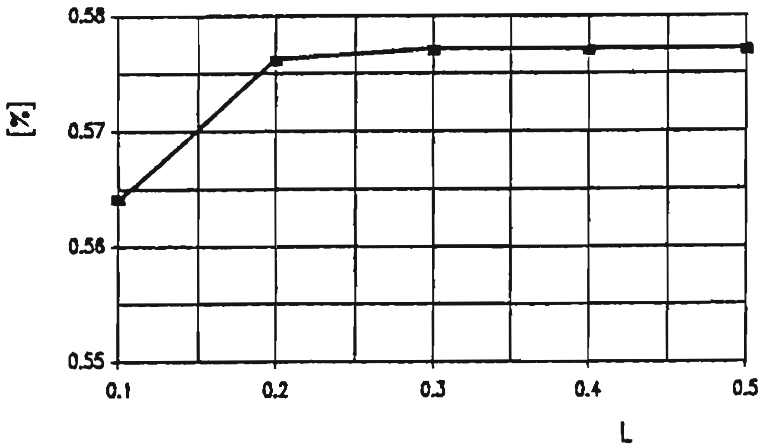

FIG. 5. Efficiency of energy recovery versus discharge factor of 34 Ah battery for angular speed change from 293 s^{-1}.

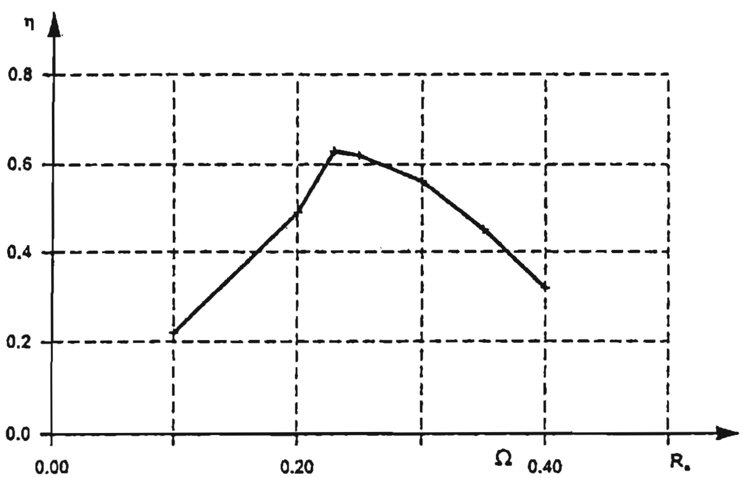

FIG. 6. Efficiency of energy recovery versus load resistance ($\omega = 293\ s^{-1}$).

The graph of energy passage efficiency versus the resistance value is given in Fig. 6. The validation of the vehicle braking energy simulation tests was carried out at the model stand (Fig. 1).

The real tests of recuperated energy amount stored in an inertia mass and passed to generator load resistors were carried out for initial angular speed

$\omega = 293\ s^{-1}$. The load current and generator voltage approached the nominal values. The load current and voltage were measured since the inertia mass reached the speed of 293 s^{-1} until it came to a standstill. The tests of recuperated energy amount passed to electrochemical batteries were carried out at the same starting angular speed of the generator. The batteries of 34 Ah capacity lined in three unit series were used (voltage 36 V).

Table 3 shows the values of currents, voltages, power and time during braking phase of the inertia mass with passing the energy to the load resistor. Table 4 shows the values of currents, voltages, power and time during braking phase of the inertia mass and storing the energy in electrochemical batteries.

Table 3. Results of studies of currents, voltages, power and time for shunt direct-current generator during inertia mass braking with energy transmission to load resistor ($\omega = 293\ s^{-1}$, $R = 0.23\ \Omega$).

t [s]	I_{obc} [A]	U [V]	P [W]	$\sum E$ [kJ]
0	60	38.6	2316	
10	50	32.0	1600	
20	39	25.0	975	
30	23	17.5	402	45.4
40	19	15.0	285	
50	10	10.0	100	
60	5.5	4.5	25	
70	0	0	0	

Table 4. Results of currents, voltages, power and time studies for series direct-current generator during inertia mass braking with energy transmission to electrochemical battery ($\omega = 293\ s^{-1}$, 34 Ah).

t [s]	I_{obc} [A]	U [V]	P [W]	$\sum E$ [kJ]
0	60	39.0	2340	
10	48	38.6	1853	
20	42	38.5	1617	44.4
30	40	38.0	1520	
40	5.0	37.0	185	
50	0	36.0	0	

Graphs of the current, voltage and power versus time for direct-current series generator during braking phase of the inertia mass and passing the energy to load resistors are shown in Fig. 7. The same parameters for the same generator obtained during the braking phase of inertia mass and storing energy in electrochemical batteries are presented in Fig. 8.

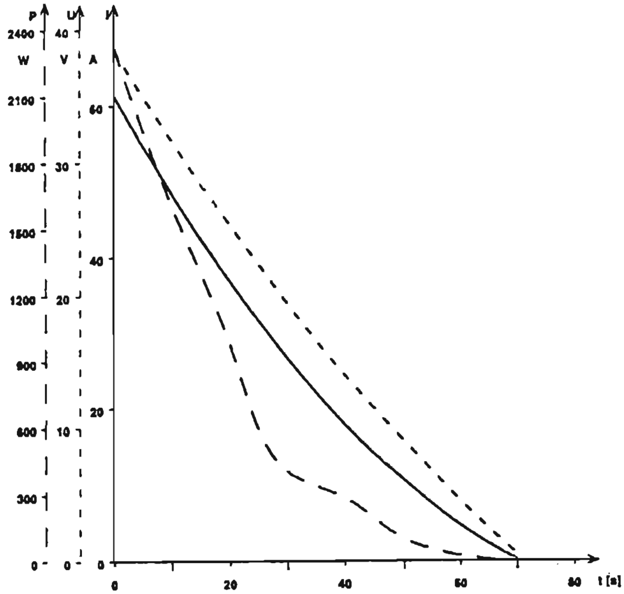

FIG. 7. Current, voltage and power versus time graphs for direct-current generator during braking phase with energy transmission to the load resistor ($\omega = 293\ s^{-1}$, $R = 0.23\ \Omega$).

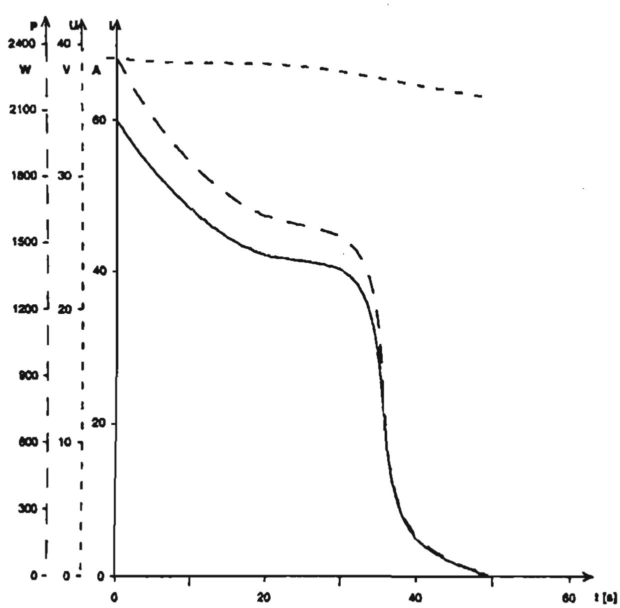

FIG. 8. Current, voltage and power versus time graphs during braking phase with energy transmission to the electrochemical battery ($\omega = 293\ s^{-1}$, 34 Ah).

3. Recuperation energy tests in automotive vehicle driving cycle

The tests and measurements of the energy to be recovered during braking phases of automobile driving cycle were carried out on the model stand with schematic diagram presented in Fig. 2. A city bus moving in accordance with the so-called Warsaw Driving Cycle [9] (Fig. 9) was chosen for the analysis. The vehicle mass was equal to 1700 kg and the range of driving cycle speeds was 25 – 50 km/h. The maximum speed during a driving cycle is 50 km/h, while the maximum angular speed of the stand generator reaches 314 s^{-1}. This angular speed corresponds to the vehicle speed of 72 km/h.

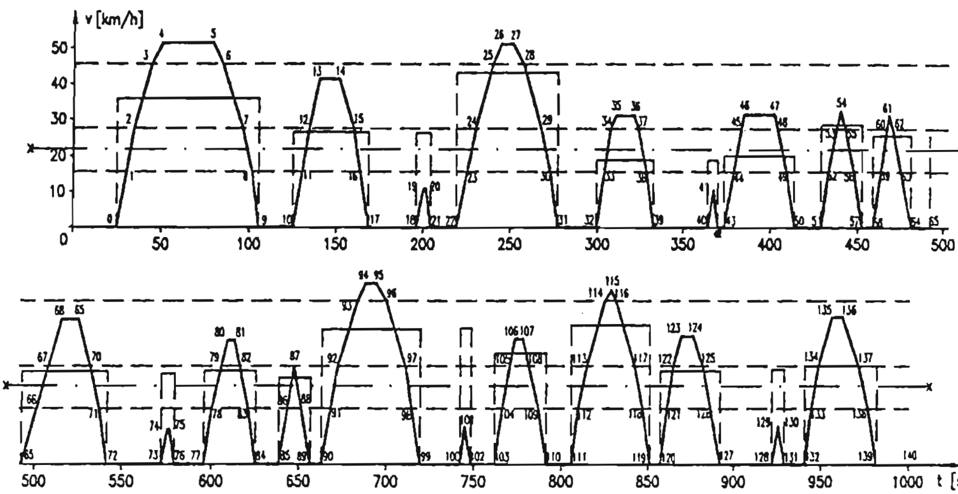

FIG. 9. Warsaw Driving Cycle: city bus speed versus time.

Assuming linear dependences of these speeds for the same periods of time, the speed ratio $72/50 = 1.44$ was introduced. On the basis of preliminary tests it was stated that for the energy recuperation process, the lower limit of the generator angular speed equals 130.8 s^{-1} (corresponding to vehicle speed of 21 km/h), as there is no energy recuperation for the speeds below this value. The consecutive measuring intervals for energy recuperation were assumed as a linear time function. These assumptions simplified the calculations.

In order to determine the real value of energy possible to be recovered, mutual proportionality of the triangle area given in driving cycle co-ordinates $V_{k(t)} = f(t_k)$ and the test stand measurement co-ordinates $W_{k(t)} = f(t_k)$ should be used. As an example, the energy analysis of the initial phases of driving cycle marked in Fig. 9 by the points $k = 5$ through 9 was performed, and the results were compared to the corresponding experimental data (Fig. 10). In the range of $k = 5$ through 9 (k – consecutive number of braking phase), the driving cycle co-

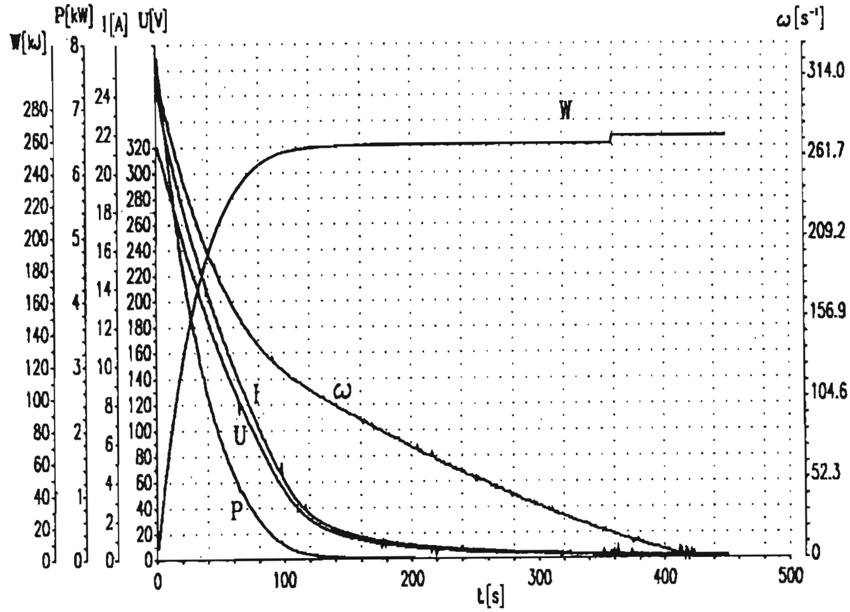

FIG. 10. Current, voltage, power, angular speed, recovered energy versus time graphs for a shunt direct-current generator during braking the inertia mass from the angular speed of 314 s^{-1}.

ordinates correspond to the following velocities: $V_{(5)} = 50$ km/h, $V_{(6)} = 42$ km/h, $V_{(7)} = 25$ km/h and $V_{(x)} = 21$ km/h. These values are related to the following angular speeds: $\omega_{(5)} = 314\ s^{-1}$, $\omega_{(6)} = 261.7\ s^{-1}$, $\omega_{(7)} = 157\ s^{-1}$, $\omega_{(x)} = 138\ s^{-1}$ obtained during the measurement experiment (Fig. 10). The period of energy supply during the driving cycle is equal to:

$$t_{(5-6)} = 8\,\mathrm{s}, \quad t_{(6-7)} = 8\,\mathrm{s}, \quad t_{(7-x)} = 4.5\,\mathrm{s}. \tag{3.1}$$

The period of energy supply during the measurements on the model stand was equal to:

$$t_{(5-6)} = 15.5\,\mathrm{s}, \quad t_{(6-7)} = 49.4\,\mathrm{s}, \quad t_{(7-x)} = 17.6\,\mathrm{s}. \tag{3.2}$$

Hence the energy amounts passed to the load resistors are as follows:

$$\begin{aligned} Wr_{(5-6)} &= \frac{8}{15.5}\,98 = 50.6\ \mathrm{kJ},\\ Wr_{(6-7)} &= \frac{8}{49.4}\,134.4 = 21.8\ \mathrm{kJ},\\ Wr_{(7-x)} &= \frac{4.5}{17.6}\,16.6 = 4.2\ \mathrm{kJ}. \end{aligned} \tag{3.3}$$

The total energy passed to the resistors equals $Wr_{(7-x)}$= 76.6 kJ, while the energy produced within the same time period on the model stand was equal to:

$$(3.4) \qquad Wp_{(5-6)} = 98\text{kJ}, \quad Wp_{(6-7)} = 134.4\text{kJ}, \quad Wp_{(7-x)} = 16.6\text{kJ}.$$

The total measured energy was equal to $Wp_{(5-x)}$ = 249 kJ. The energy to be recovered during braking phases of the whole driving cycle can be calculated in a similar way.

4. Testing the energy recuperation during duty cycles of heavy machinery working and driving systems

Tests and measurements of the energy possible to be recovered during braking phases (lowering of the loaded sheave block) of the working and driving systems of the self-propelled crane were carried out on model stand with schematic diagram shown in Fig. 3. The self-propelled crane operating cycle is of a different type, where the combustion engine supplies power either for carrying the loads or for moving the crane.

The analysed crane DUT-0300, driven by a 178.5 kW combustion engine and with lifting capacity of 30 Mg, during the exemplary working mechanisms cycle (reach 3.0 m, lifted mass 30 Mg, telescopic length 8.5 m) yielded the theoretical possibility to recover the energy of 1384 kJ in the loaded sheave block lowering phase. This phase lasted 28.6 s. During the on-road driving cycle phase, the two-step braking occurred: from the speed of 60 km/h to 35 km/h, and from 35 km/h to 0 km/h. The first braking phase lasted 11 seconds with the theoretically recoverable energy of 1770 kJ. The second braking phase lasted 15 seconds, while the theoretically recoverable energy was 925 kJ. The exemplary results of recuperation energy studies for working mechanism cycles correspond to the experiments shown in Table 5.

Table 5. Results of energy recuperation during operating cycle of crane working mechanisms.

Measurement number	Generator angular speed	Generator loading current	Generator voltage	Energy recovered	Experiment time	Energy recuperation factor
-	s^{-1}	A	V	kJ	s	kJ/s
1	298.3	10.8	236	275	110	2.5
2	290.4	13.0	273	395	110	3.6

The calculated factor of energy recovery W_p determines the amount of energy to be recovered within 1 s of lowering phase of a loaded sheave block. The factor value depends on the level of the power supplied at the moment start of the experiment to the generator installed on the model stand. The first experiment (Table 5) shows the test results for the generator reaching the power of 2.5 kW (generator's nominal power). The graphic representation of the tests is shown in Fig. 11. On the basis of the experiment results analysis it may be stated that:

- the generator power $P_1 = 2.5$ kW (nominal power),
- the recovered energy $W_1 = 275$ kJ,
- the experiment time period $t_1 = 110$ s,
- the recovered energy factor $w_{p1} = \dfrac{W_1}{t_1} = 2.5\ \dfrac{\text{kJ}}{\text{s}}$.

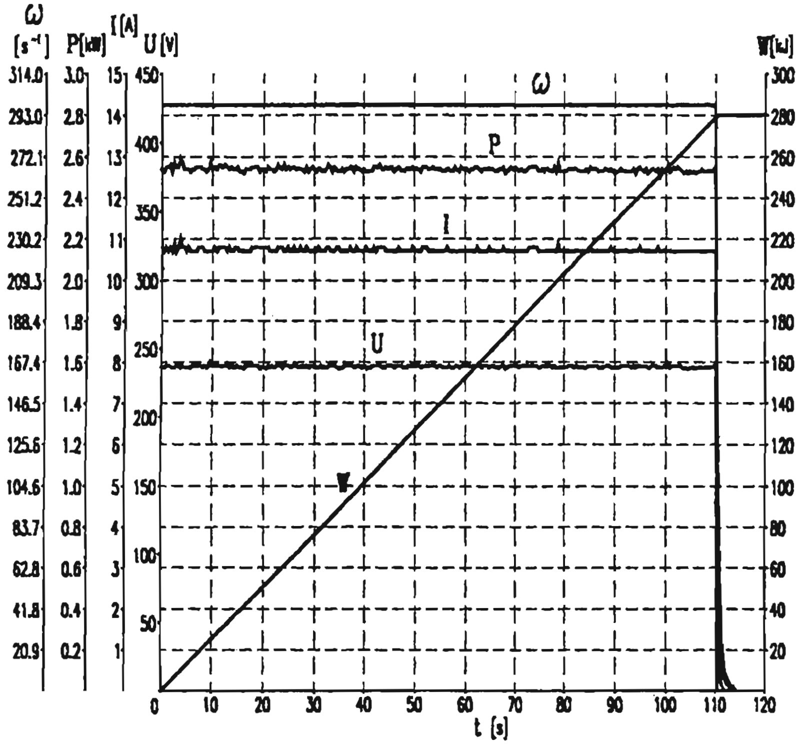

FIG. 11. Current, voltage, power, angular speed and recovered energy versus time graphs for shunt direct-current generator during loaded sheave block lowering phase ($\omega = 298.3$ s^{-1}, $P = 2.5$ kW).

In this case the factor w'_{p1}, represented by the ratio of the recovered energy factor to the power supplied to generator at the starting point of the experiment, is a general factor (power P_1 equals the nominal power) equal to $w'_{p1} = 1$.

For the experimental data transformation to a real object it was assumed, that the generator installed in the measurement chain has the nominal power of 48.4 kW. In such a case, the following relation should be used to estimate the

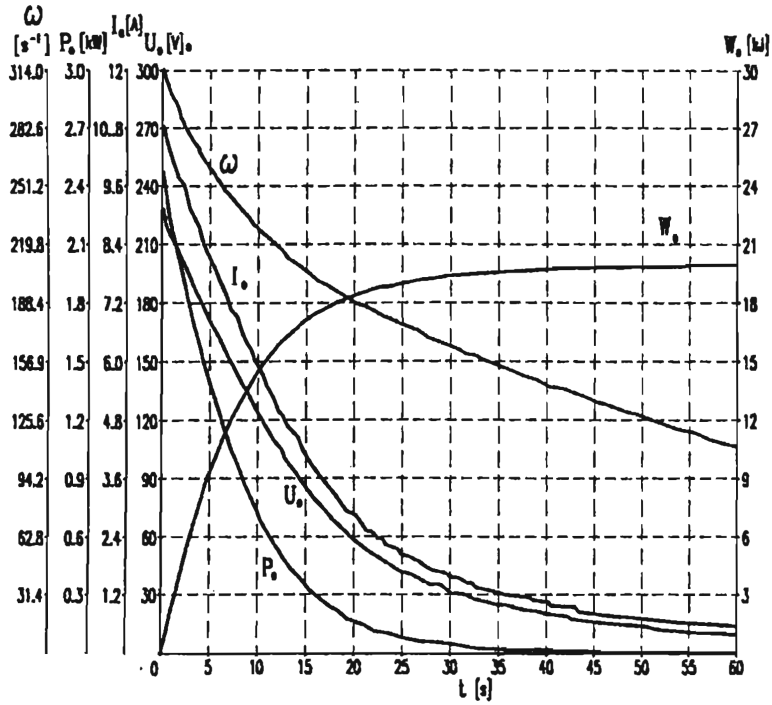

FIG. 12. Current, voltage, power angular speed and recovered energy versus time for shunt direct-current generator during braking the inertia mass from the angular speed of 314 s^{-1}.

energy possible to recover on the real object:

$$\frac{w'_{p1} \cdot P_n}{P_1} \cdot t_n \cdot w_{p1} = \frac{1 \cdot 48.4}{2.5} \cdot 28.6 \cdot 2.5 = 1384.2 \text{ kJ} , \tag{4.1}$$

where P_n – the nominal power of the generator in the real object, t_n – the loaded sheave block lowering time for the real object.

It follows from the results of experiment no. 2, that:

- the generator power $P_2 = 3.6$ kW (exceeds the nominal power),
- the energy recovered $W_2 = 395$ kJ,
- the experiment time $t_2 = 110$ s,
- the recovered energy factor $w_{p2} = 3.6 \frac{\text{kJ}}{\text{s}}$.

In this case $w'_{p2} = 1.44$. This factor defines the overload capacity degree of the generator installed on the test stand or it shows the rise of the recovered energy in real object, if the nominal power is increased by this factor. The calculations of the energy recovered at the real object under the above mentioned conditions are made according to the following equation:

$$\frac{w'_{p2} \cdot P_n}{P_2} \cdot t_n \cdot w_{p2} = \frac{1.44 \cdot 48.4}{3.6} \cdot 28.6 \cdot 3.6 = 1993.3 \text{ kJ} . \tag{4.2}$$

In practice, the direct-current generator with nominal power of 25 kW would be installed on the real object. Then, by analysing the lowering phase of the crane working mechanisms cycle using, for example, the results obtained during the experiment no. 1, and maintaining the real lowering times of the loaded sheave block, the recovered energy may be calculated as follows:

$$\frac{w'_{p1} \cdot P_n}{P_2} \cdot t_n \cdot w_{p1} = \frac{1 \cdot 25}{2.5} \cdot 28.6 \cdot 2.5 = 715 \text{ kJ} . \tag{4.3}$$

According to Fig. 11, the characteristics correspond to the 2.5 kW generator. The tests results formed the background for calculations of the energy recovered during braking phases of the on-road driving cycle. It was assumed that the 60 km/h speed corresponds to generator angular speed of 314 s^{-1}. Furthermore, the generator angular speed equal to 157 s^{-1} (corresponding to the driving speed of 30 km/h) was considered as the lower limit for energy recovery. The linear dependence of angular speed and linear speed on time was assumed in the calculations. In the analysed part of the on-road driving cycle for $k = 1$ through 2 and $k = 3$ through 4, the co-ordinates of driving cycle have the following values:

$$V_{C(1)} = 60 \text{ km/h}, \quad V_{C(2)} = 35 \text{ km/h}, \quad V_{C(3)} = 35 \text{ km/h} \text{ and } V_{C(4)} = 30 \text{ km/h},$$

while the measurement co-ordinates reach the values:

$$\omega_{p(1)} = 314s^{-1}, \quad \omega_{p(2)} = 183.1\text{s}^{-1}, \quad \omega_{p(3)} = 183.1\text{s}^{-1} \text{ and } \omega_{p(4)} = 157\text{s}^{-1}.$$

The energy supply times, registered on the test stand, are

$$t_{p(1-2)} = 22.4 \text{ s}, \quad t_{p(3-4)} = 11.6 \text{ s}.$$

With the stand generator power of 2.5 kW and the stand inertia mass selected to maintain the ratio of its kinetic energy at angular speed of 314 s^{-1} to kinetic energy of a crane moving at 60 km/h equal to 1:32, the obtained values of energy relating to the real object were as follows:
for $k = 1$ to 2

$$22.4 \cdot \times 12.5 \cdot \times 32 = 1792 \text{ kJ},$$

for $k = 3$ to 4

$$11.6 \cdot \times 2.5 \cdot \times 32 = 928 \text{ kJ}.$$

5. Concluding remarks

The following conclusions may be drawn from the considerations presented in the paper:

- there exists the possibility to recover the energy during braking phases of the automobile or heavy machine movement as well as during lowering process of the loaded crane sheave block;
- mechanical energy of braking the classically driven automobiles or lowering the loaded sheave block of heavy machinery, transformed into electric energy, may be utilised for charging the electrochemical batteries or for supplying the heating resistors, working as an additional heat energy source;
- the mechanical-into-electric energy transducers for both the model stands and real objects are the direct-current or alternating-current generators;
- for both the automobiles and the heavy machinery, the recovered energy transformed into heat energy can be used for regeneration of ecological devices, such as soot filters or catalytic converters.

References

1. J. Ocioszyński, *Energy saving in vehicles with electric and hybrid electromechanical drive systems* [in Polish], WPW, Prace Naukowe – Mechanika, 96, 1986.
2. K. Michałowski, J. Ocioszyński, *Electric and hybrid driven automobiles*[in Polish], WKiŁ, Warszawa 1989.
3. J. Ocioszyński, *Electroenergy studies of hybrid electromechanical vehicles drive systems* [in Polish], WPW, Prace Naukowe – Mechanika, 76, 1981.
4. J. Ocioszyński, *Power engineering of heavy machinery energy-saving drive systems* [in Polish], OWPW, Warszawa 1994.
5. P. Majewski, J. Ocioszyński, *The experimental stand – property studies of a hybrid drive system* [in Polish], Instytut Maszyn Roboczych Ciężkich Politechniki Warszawskiej, Warszawa 1984.
6. P. Majewski, J. Ocioszyński, *The experimental stand with an automatic control and power parameters recording system* [in Polish], Problemy Eksploatacji 2/97, Kwartalnik Naukowy Instytutu Technologii Eksploatacji .
7. P. Majewski, *Research Project No. 7 TO7C 03114 Electro-energy studies of ecology devices for toxic exhausts components limitation of heavy machinery* [in Polish],
8. E. Koziej, *Electric machines in automobiles* [in Polish], WNT, Warszawa 1986.
9. A. Szumanowski, *Energy accumulation in vehicles* [in Polish], WKiŁ, Warszawa 1983.

Received February 28, 2001.